Journal of Applied Electrochemistry **30**: 1351–1360, 2000.

Determination of diffusion coefficients of depositing ions in molten chlorides by transient electrochemical techniques†

T. STØRE[1]*, G.M. HAARBERG[2] and R. TUNOLD[1]
[1]*Department of Materials Technology and Electrochemistry, Norwegian University of Science and Technology, N-7491 Trondheim, Norway*
[2]*SINTEF Materials Technology, N-7465 Trondheim, Norway*
*(*author for correspondence, e-mail: trond.store@hydro.com, Present address: Hydro Aluminium Technology Centre Årdal, N-6882 Øvre Årdal)*

Received 31 July 1999; accepted in revised form 25 April 2000

Key words: diffusion coefficient, electrodeposition, molten chlorides, transient techniques

Abstract

The electrochemical reduction of Pb(II), Zn(II) and Mg(II) ions at glassy carbon and tungsten electrodes in molten KCl–LiCl eutectic was studied by linear sweep voltammetry (LSV), convolutive potential sweep voltammetry (CPSV), chronopotentiometry and chronoamperometry. In the case of lead deposition, the initial nucleation stage was found to influence the shape of the voltammetric current peak. CPSV was consequently believed to be a more reliable method than LSV for the calculation of the diffusion coefficient of the Pb(II) ion. Similar complications were not observed for zinc and magnesium since the nucleation overpotentials for these metals were significantly lower than for lead. On the other hand, lithium codeposition made it difficult to interpret the zinc and especially the magnesium convolution voltammograms. Chronopotentiometry yielded practically identical results for $D_{Pb(II)}$ as the voltammetric techniques. However, due to a substantial residual current, the Sand equation was not obeyed for the Zn(II) and Mg(II) ions. Determination of diffusion coefficients from single potentiostatic current transients and the Cottrell equation was not found to be a very reliable method. Empirical expressions for the temperature dependence of D in the range 400–500 °C were calculated for all three ions.

List of symbols

c^{∞}	bulk concentration (mol cm^{-3})
D	diffusion coefficient (cm^2 s^{-1})
E	potential (mV)
E_p^C	cathodic peak potential (mV)
E_{rev}	reversible potential (mV)
F	faradaic constant (96 487 C mol^{-1})
I	current (mA)
I_r	residual current (mA)
i	current density (mA cm^{-2})
i_p^C	cathodic peak current density (mA cm^{-2})
i_r	residual current density (mA cm^{-2})
m	convoluted current density (mA cm^{-2} s$^{1/2}$)
m_{∞}^C	cathodic limit of convoluted current density (mA cm^{-2} s$^{1/2}$)
n	number of electrons in overall reaction
R	gas constant (8.3143 J mol^{-1} K^{-1})
T	temperature (K)
t	time (s)

Greek symbols

η	overpotential (mV)
v	potential sweep rate (mV s^{-1})
τ	transition time (s)
Φ	Dawson's integral

1. Introduction

Molten alkali chlorides may be regarded as simple ionic liquids. Their strong ionic dissociation together with the elevated temperatures result in high conductivities and charge transfer rates. Under such conditions it is found that practically all electrode reactions are mass transfer controlled. Exceptions to this rule are processes which involve the formation of a new phase, of which metal deposition on solid electrodes is a typical example. The rate of such electrocrystallization processes is initially determined by the frequency of appearance of stable growth centres (i.e., the nucleation rate).

In voltammetry, which is probably the most widely employed transient electrochemical technique, the nucleation step may cause a sweep rate dependence of the peak potential. To see how this occurs, consider the general metal deposition reaction

† Dedicated to the memory of Daniel Simonsson

$$M^{n+} + ne^- = M \quad (1)$$

The current response to a linear potential sweep at a solid electrode is described by the following equation, which was first derived by Berzins and Delahay [1]:

$$i = -\frac{2}{\pi^{1/2}}\frac{(nF)^{3/2}}{(RT)^{1/2}}D^{1/2}c^{\infty}v^{1/2}\Phi\left[\left(\frac{nF}{RT}vt\right)^{1/2}\right] \quad (2)$$

where

$$\Phi(x) = \exp(-x^2)\int_0^x \exp(t^2)\mathrm{d}t \quad (3)$$

is known as Dawson's integral, with a maximum value of 0.5410 for $x = 0.9241$ [2]. Thus the cathodic peak current density

$$i_p^C = -0.6105\frac{(nF)^{3/2}}{(RT)^{1/2}}D^{1/2}c^{\infty}v^{1/2} \quad (4)$$

occurs at the peak potential given by

$$E_p^C = E_{rev} - 0.8540\frac{RT}{nF} \quad (5)$$

To simplify the mathematical treatment, Berzins and Delahay considered only the case with a constant activity of M equal to unity. This hypothesis is obviously not justified unless the electrode is covered by at least one monolayer of the deposit. In essence it is thus assumed that the transition from a bare to a completely covered electrode occurs in close vicinity to the reversible potential. However, the total charge passed in a sweep decreases with increasing sweep rate, so that at sufficiently high sweep rates this assumption is no longer valid. The reduced surface coverage results in a broader peak and a displacement of the peak potential towards more cathodic values. Furthermore, a departure from linearity between the peak current density and the square root of sweep rate will be observed. This behaviour is sometimes interpreted incorrectly as slow kinetics.

The main purpose of this work is to investigate the applicability of various transient electrochemical techniques for the determination of diffusion coefficients during metal deposition on solid electrodes in molten alkali chlorides. It will be demonstrated that the voltammetric peak current density may be influenced by the nucleation step even at moderate sweep rates. This of course has a direct effect on the calculation of the diffusion coefficient. A similar conclusion was reported by Hills et al. [3], who studied the electrodeposition of silver from molten KNO_3–$NaNO_3$. It will be shown that under such circumstances, a more reliable result may be obtained from the limiting value of the convoluted current density. Furthermore, it will be demonstrated that codeposition of alkali metals results in a residual current that is more easily dealt with in voltammetry than in either chronopotentiometry or chronoamperometry.

The paper also offers quantitative data for the diffusion of Pb(II), Zn(II) and Mg(II) ions in molten KCl–LiCl eutectic. Empirical expressions for the temperature dependence of the diffusion coefficients in the range 400–500 °C will be presented. Previously the electrochemistry of $PbCl_2$ [4–10] and $ZnCl_2$ [9–12] in KCl–LiCl have been studied by a number of authors. However, at least to the authors knowledge, no comprehensive investigation of the electrochemistry of $MgCl_2$ in this solvent has been published.

2. Experimental details

All experiments were carried out in an inert argon atmosphere inside a VAC model HE-43-2 glove box with a purification system capable of oxygen and moisture removal to less than 1 ppm. Dry analytical grade chloride salts (Merck) were prepared prior to the experiments and stored in the glove box. KCl and LiCl were dried under vacuum at 500 °C for about 12 h. $PbCl_2$, $ZnCl_2$ and $MgCl_2$ were distilled under vacuum in a single-stage batch process. Prior to the distillation, anhydrous $MgCl_2$ was prepared by slowly heating $MgCl_2 \cdot 6\,H_2O$ to 450 °C under HCl atmosphere (to avoid hydrolysis).

A eutectic mixture of KCl and LiCl (0.405:0.595) served as base electrolyte. The dilute solution of either $PbCl_2$ (0.0306 M), $ZnCl_2$ (0.0312 M) or $MgCl_2$ (0.310 M) was contained in a 50×50 mm glassy carbon crucible. Temperature regulation within ± 2 °C was achieved with a Eurotherm model 2404 temperature controller and a calibrated type S thermocouple (Pt/Pt − 10%Rh).

The working electrode in the lead and zinc experiments was a pyrex-sheathed glassy carbon rod, while a similar tungsten rod was used in the magnesium experiments. The geometrical area of these disk electrodes was 0.071 cm^2. Each electrode surface was polished to a mirrorlike finish with SiC paper and 1 μm diamond paste. A glassy carbon rod served as counter electrode. A metal/metal ion electrode corresponding to the system under investigation was used as reference electrode. The Pb(II)/Pb and Zn(II)/Zn reference electrodes consisted of a pool of liquid metal in a quartz tube. A slot about 5 mm above the metal surface allowed the molten electrolyte to flow into the tube. The Mg(II)/Mg reference electrode was a cylinder of solid magnesium in direct contact with the melt.

The electrochemical measurements were executed with a Radiometer DEA-I digital electrochemical analyser. Signal imposition and data acquisition were handled by the Windows-based VoltaMaster 2 integrated software. The potentiostat contained a positive feedback circuit for ohmic drop compensation. It was generally found impossible to apply the feedback value suggested by the

software without the onset of potentiostat oscillations. The compensation was thus performed to the maximum extent allowed by the potentiostat.

3. Results and discussion

3.1. *Voltammetry*

Figure 1 shows two consecutive cyclic voltammograms for lead deposition on glassy carbon. In both cases the potential was swept at 100 mV s^{-1} from +500 mV (open circuit) to −500 mV and back to +500 mV. The electrode was held at open circuit for five minutes prior to each measurement. Curve A was preceded by a similar potential scan (not shown in the Figure) where the reverse sweep was continued to +1000 mV before returning to open circuit.

Interestingly, the shapes as well as the positions of these cathodic peaks are quite different. In particular, although the same sweep rate was applied for both curves A and B, the peak current densities are not equal. The observed differences may be explained as follows. The voltammetric theory, represented by Equations 2 and 5, presupposes that the deposition starts at the reversible potential (given by the Nernst equation). However, because the deposition of Pb on a foreign substrate such as glassy carbon requires a significant overpotential, the actual deposition potential is considerably more cathodic than E_{rev}. Moreover, once the current starts flowing the concentration gradient of Pb(II) ions at any given potential will be steeper than if the deposition had started at E_{rev}. As a consequence the observed peak current density will be higher than expected by theory. This behaviour was also observed by Hills et al. [3].

The two peak current densities in Figure 1 differ by 23%. It follows that a calculation of the diffusion coefficient with Equation 4 yields two results which differ by as much as 51%. Rather than analysing only the current peak, it is desirable to use all the information contained in the voltammograms. One such method is convolutive potential sweep voltammetry (CPSV) [13], also referred to as semi-integral electroanalysis [14]. The key aspect of this technique is that the convoluted (semi-integrated) current density

$$m(t) = \frac{d^{-1/2}}{dt^{-1/2}} i(t) = \frac{1}{\pi^{1/2}} \int_0^t \frac{i(u)}{(t-u)^{1/2}} du \tag{6}$$

will reach a limiting value given by

$$m_\infty^C = -nFD^{1/2}c^\infty \tag{7}$$

provided the potential becomes sufficiently cathodic to ensure complete concentration polarization of the reactant (i.e., zero surface concentration).

Figure 2 shows the result of semi-integrating the cyclic voltammograms in Figure 1. The limiting values m_∞^C (mA cm^{-2} $s^{1/2}$) correspond to the plateaus in the cathodic branches. They are practically identical because the voltammograms in Figure 1 eventually converge. The convolution voltammograms do not retrace themselves on the reverse sweep as would be expected of a reversible process. It should be obvious by now that the nucleation overpotential is the source of this irregular behaviour. Therefore the forward curves do not superimpose, whereas the reverse sweeps intersect the potential axis together at the origin.

It should be noted that the value of the diffusion coefficient calculated from m_∞^C corresponds to the peak current density in curve B. In this voltammogram the deposition starts at −20 mV. In curve A, however, the deposition does not start until an overpotential of −70 mV is reached. The reason for this is not fully understood, but apparently the nucleation process becomes retarded by sweeping sufficiently far in the anodic direction. What is important here is that unrealistic values of the diffusion coefficient will be obtained in the presence of a large nucleation overpotential. This

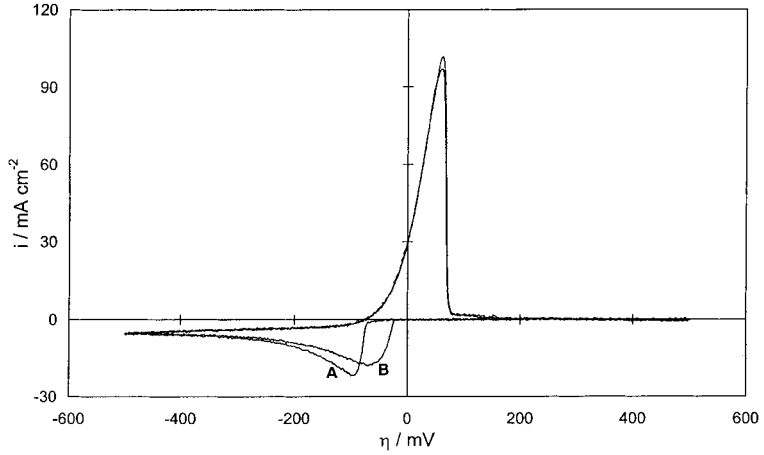

Fig. 1. Cyclic voltammograms for the deposition of Pb on glassy carbon. Curves A and B are preceded by scans with anodic switching potential of +1000 mV and +500 mV, respectively. Sweep rate 100 mV s^{-1}. Temperature 400 °C. [$PbCl_2$] = 0.0306 M.

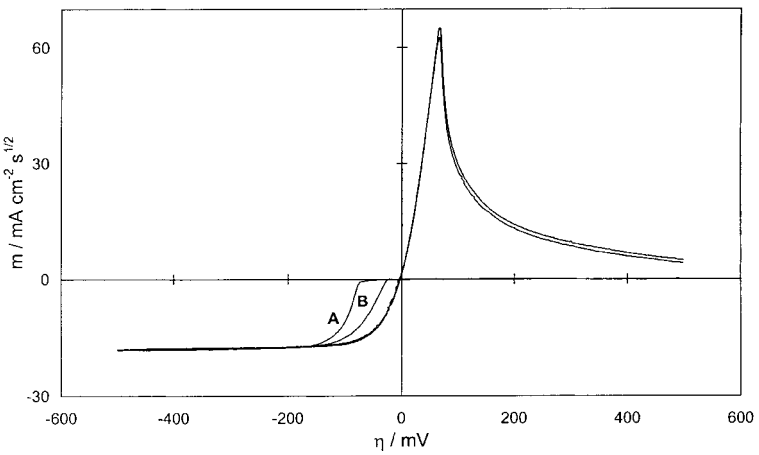

Fig. 2. Semi-integration of the cyclic voltammograms in Figure 1.

was avoided by terminating the sweep at the open circuit potential.

The Pb(II), Zn(II) and Mg(II) reduction processes were studied by cyclic voltammetry over a wide range of sweep rates in the temperature interval 400–500 °C. A representative selection of voltammograms for the deposition of zinc on glassy carbon is displayed in Figure 3. Note that a correction has been made due to a substantial residual current observed prior to the Zn(II) reduction peak. This background current, which was linear with E, made the voltammograms appear tilted. Subtraction of the residual current was thus tantamount to 'lifting' the voltammograms to a horizontal position, so that the background current served as baseline for the Zn(II) reduction peak. A similar but much less pronounced residual current was observed in the Mg voltammograms, whereas no correction of the Pb voltammograms was necessary. The appearance of a shoulder on the anodic stripping peak is probably due to the oxidation of alkali metal intercalated in the lattice of the glassy carbon electrode.

Figure 4 shows the sweep rate dependence of the cathodic peak current density for the reduction of the three ions at 400 °C. The plots are normalized with respect to concentration in order to make a direct comparison. In all cases a linear relation was found between i_p^C and $v^{1/2}$ for $v \leq 2000$ mV s^{-1}, whereas a significant departure from linearity was observed at higher sweep rates. The deviation at 10000 mV s^{-1} increased in the order Zn(4%), Mg(13%) and Pb(20%). As discussed above, the reason for these deviations is probably that the assumption of constant unit activity of the deposit fails at high sweep rates.

The diffusion coefficients of the Pb(II), Zn(II) and Mg(II) ions at 400 °C were calculated from the slopes of the regression lines and Equation 4. The results are collected in Table 1. The cathodic limit in the Pb convolution voltammograms was found to be essentially independent of sweep rate, with an average value of $m_\infty^C = -17.59$ mA cm^{-2} s$^{1/2}$. Inserting this value in Equation 7 yields $D_{Pb(II)} = 0.89 \times 10^{-5}$ cm^2 s^{-1}. As seen from Table 1, this result is in excellent agreement with the value 0.88×10^{-5} cm^2 s^{-1} obtained by linear sweep voltammetry. The main advantage of the CPSV technique over LSV is that it is not sensitive to the magnitude of the nucleation overpotential.

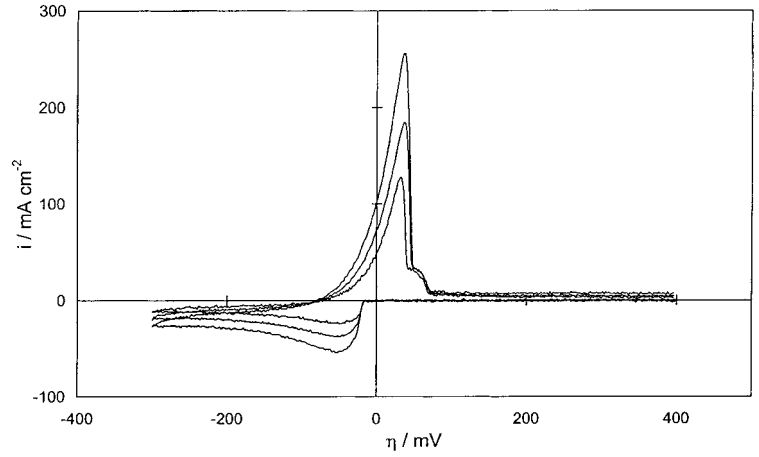

Fig. 3. Cyclic voltammograms for the deposition of Zn on glassy carbon. Sweep rates 200, 500 and 1000 mV s^{-1}. Temperature 400 °C. [$ZnCl_2$] = 0.0312 M.

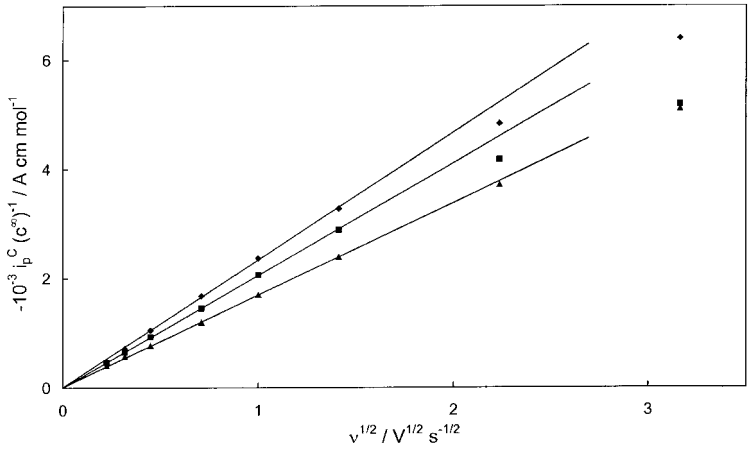

Fig. 4. Concentration normalized cathodic peak current density against square root of sweep rate. Temperature 400 °C. $[PbCl_2]$ = 0.0306 M; $[ZnCl_2]$ = 0.0312 M; $[MgCl_2]$ = 0.3101 M. key: (◆) Mg, (■) Pb, (▲) Zn.

Table 1. Diffusion coefficients of the Pb(II), Zn(II) and Mg(II) ions in KCl–LiCl eutectic at 400 °C

Technique	10^5 D/cm^2 s^{-1}		
	Pb(II)	Zn(II)	Mg(II)
Linear sweep voltammetry	0.88	0.59	1.13
Convolution voltammetry	0.89	0.60	–
Chronopotentiometry	0.85	(1.24)	(1.39)
Potential step	1.01	1.06	–

Figure 5 shows the Zn convolution voltammograms corresponding to Figure 3. They are independent of sweep rate and therefore superimpose. Unfortunately the determination of m_∞^C is complicated by the fact that the 'plateaus' are not quite horizontal. Such sloping curves are fairly common and are sometimes ascribed to nonfaradaic currents or sphericity effects [14]. However, these effects cannot account for the difference between the Zn and Pb convolution voltammograms in the present case.

A similar behaviour would be expected in the event of a parallel reaction. Codeposition of lithium is thus a plausible explanation for the sloping Zn convolution voltammograms. On the assumption that the Li deposition current increased linearly with potential, it is possible to subtract it from the voltammograms before the semi-integration. The subtracted amount was gradually increased until a horizontal plateau was obtained in the forward sweep, as demonstrated in Figure 6. This trial and error procedure is obviously somewhat arbitrary, but as it turned out it yielded $D_{Zn(II)} = 0.60 \times 10^{-5}$ cm^2 s^{-1}, which again is in excellent agreement with the value 0.59×10^{-5} cm^2 s^{-1} obtained by linear sweep voltammetry (cf. Table 1).

Magnesium is a considerably less noble metal than lead and zinc. The standard potential of the Mg(II)/Mg couple is approximately 1.0 V more negative than the Zn(II)/Zn couple in eutectic KCl–LiCl [15]. Li codeposition is consequently expected to be even more pronounced during Mg deposition than during Zn deposition. A typical cyclic voltammogram for the deposition of Mg on tungsten and its corresponding convolution voltammogram are shown in Figure 7. The forward sweep of the latter resembles the Zn convolution voltammograms in Figure 5 in so far as the

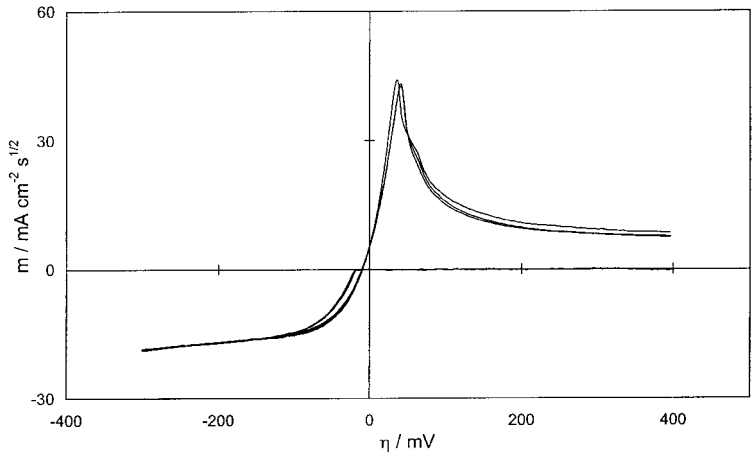

Fig. 5. Semi-integration of the cyclic voltammograms in Figure 3.

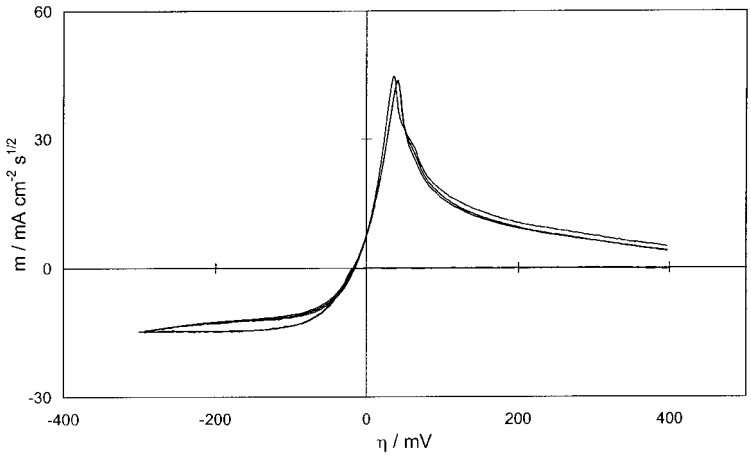

Fig. 6. Same as Figure 5, but with correction for Li codeposition before the semi-integration.

convoluted current density grows steadily with potential. However, it is not retraced by the reverse sweep.

A similar but less pronounced convolution voltammogram was obtained by Castrillejo et al. [16] in equimolar $CaCl_2$–NaCl. Because the forward and reverse sweeps were not identical, they concluded that the Mg(II) reduction was not a reversible reaction. It must be emphasized that slow kinetics of the electrode reaction cannot account for the lack of a plateau in the cathodic branch of the convolution voltammogram in Figure 7. As mentioned above, complete concentration polarization of the reactant is the only prerequisite for the convoluted current density to reach a limiting value given by Equation 7 [14]. However, if another species is reduced in a parallel process, $m(t)$ is expected to grow until this second species also becomes depleted.

The fact that some underpotential deposition of Li takes place beyond the Mg reduction peak was even more evident at lower sweep rates. Figure 8 shows a cyclic voltammogram with a sweep rate of 100 mV s^{-1}. A current increase due to Li deposition occurred just before the switching potential was reached, even though this was less cathodic than in the 1000 mV s^{-1} voltammogram in Figure 7. Apparently the codeposition of Li was facilitated by a larger amount of deposited Mg. On the other hand, Figure 4 shows that the peak current density was not affected by Li codeposition. Linear sweep voltammetry was consequently a more suitable technique than convolution voltammetry for the calculation of the diffusion coefficient of the Mg(II) ion.

3.2. *Chronopotentiometry*

Chronopotentiometry was employed in the further study of the Pb(II), Zn(II) and Mg(II) reduction processes. Some typical chronopotentiograms for the deposition of Zn on glassy carbon are shown in Figure 9. Perhaps the most noticeable feature of these E/t curves is the rather slow transition to potentials determined by the Zn/Zn(II) couple. Initially the potential of the working electrode was governed by the same reaction that was responsible for the residual current in the cyclic voltammograms.

The Sand equation

$$i\tau^{1/2} = -\frac{\pi^{1/2} n F D^{1/2} c^{\infty}}{2} \tag{8}$$

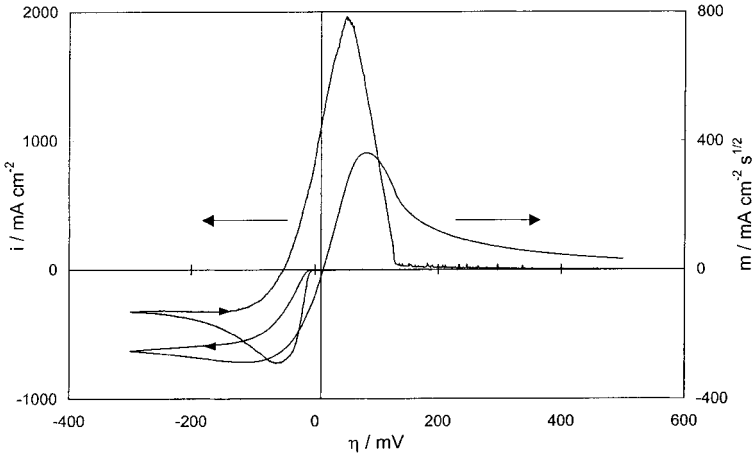

Fig. 7. Cyclic voltammogram with corresponding convolution voltammogram for the deposition of Mg on tungsten. Sweep rate 1000 mV s^{-1}. Temperature 400 °C. [$MgCl_2$] = 0.3101 M.

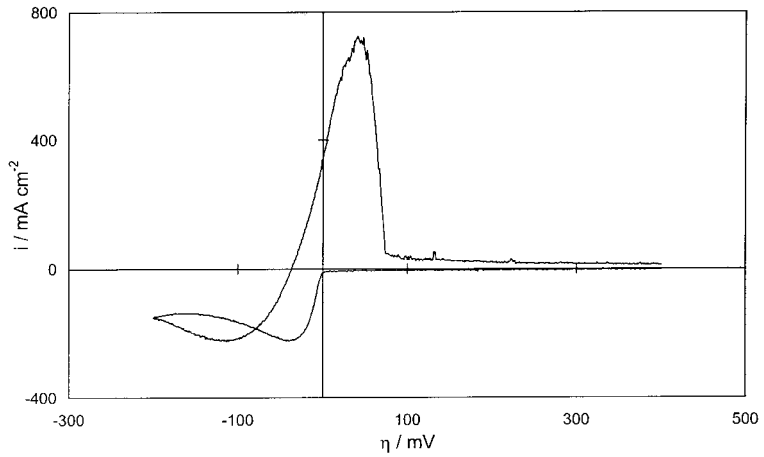

Fig. 8. Cyclic voltammogram for the deposition of Mg on tungsten. Sweep rate 100 mV s^{-1}. Temperature 400 °C. [$MgCl_2$] = 0.3101 M.

predicts that the product $i\tau^{1/2}$ should be independent of the applied current. This is frequently used as a diagnostic test for a diffusion controlled process [17]. It is evident from Figure 10 that although $i\tau^{1/2}$ tends to approach a limit at high currents, Equation 8 is far from obeyed for the Zn(II) reduction. Also Yurkinskii and Makarov, who studied the reduction of Pb(II) ions in KCl–LiCl, found that $i\tau^{1/2}$ increased with decreasing applied current [8].

Generally, a failure to meet the aforementioned criterion might indicate the presence of coupled homogeneous chemical reactions, adsorption or measurement artifacts such as double-layer charging or convection [18]. In the present case, however, the following explanation may be given. It might be recalled that the voltammetric peak currents were measured against the baseline defined by the extension of the background current. This is a well-established procedure in the analysis of voltammograms. Clearly some sort of adjustment must be made also in chronopotentiometry in order to take the residual current into account.

The problem with chronopotentiometry is that the fraction of the applied current consumed by a parallel reaction cannot be observed directly. As the background current in the voltammograms was only a weak function of potential, a natural approach was to subtract a constant I_r from the applied currents. For the Zn(II) reduction, the best fit to the Sand equation was obtained by setting $I_r = -0.53$ mA. As demonstrated in Figure 10, the product $(i - i_r)\tau^{1/2}$ was found to be independent of applied current, with an average value equal to -18.75 mA cm^{-2} $s^{1/2}$. Inserting this value into Equation 8 yields $D_{Zn(II)} = 1.24 \times 10^{-5}$ cm^2 s^{-1}, that is, more than twice the value obtained by linear sweep voltammetry (cf. Table 1). It is indeed contradictory that the transition times for Zn(II) reduction were longer than for Pb(II) reduction while the peak currents were lower.

Treating the results for the Mg(II) reduction process in a similar fashion yielded $D_{Mg(II)} = 1.38 \times 10^{-5}$ cm^2 s^{-1}. In this case the deviation from the result obtained by LSV is not more than 22%, which for practical purposes might be considered to be sufficiently accurate. The improved agreement is expected because the Mg(II) concentration was approximately ten times higher than the Zn(II) concentration, thus reducing the relative magnitude of the residual current. Nevertheless, in view

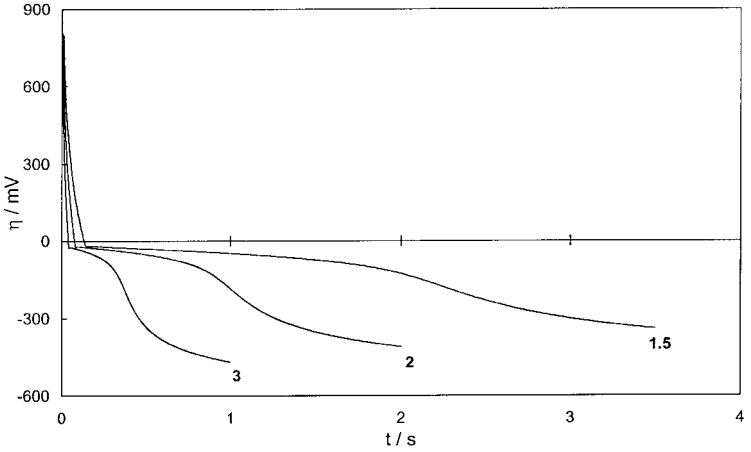

Fig. 9. Chronopotentiograms for the deposition of Zn on glassy carbon. The numbers in the figure refer to applied currents (mA). Temperature 400 °C. [$ZnCl_2$] = 0.0312 M.

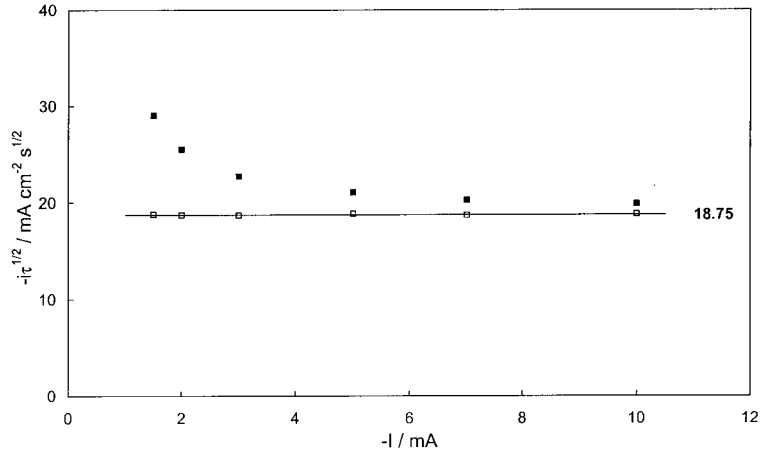

Fig. 10. Plot of $i\tau^{1/2}$ (filled squares) versus applied current for the deposition of Zn on glassy carbon. The horizontal line and the numerical value represent the average of the adjusted experimental points (open squares). See text for explanation. Temperature 400 °C. [$ZnCl_2$] = 0.0312 M.

of these discrepancies and the fact that the procedure of subtracting a constant I_r from the applied current is somewhat arbitrary, one can conclude that chronopotentiometry is less suited than voltammetry in the presence of large residual currents. For the Pb(II) reduction process, however, the residual current was negligible. Consequently, no adjustments were necessary, and as seen from Table 1 the result $D_{Pb(II)} = 0.85 \times 10^{-5}$ cm^2 s^{-1} is in excellent agreement with the two voltammetric values.

3.3. *Chronoamperometry*

In studies of electrochemical nucleation the diffusion coefficient is needed for the calculation of number densities of nuclei. Traditionally, D has been obtained from single potentiostatic current transients at high overpotentials [19]. Provided the potential is stepped to a value where the surface concentration of the reactant is effectively zero, the current density at long times will fall as $t^{-1/2}$ according to the Cottrell equation:

$$i = -\frac{nFD^{1/2}c^{\infty}}{\pi^{1/2}t^{1/2}} \tag{9}$$

For a two electron metal deposition process at 400 °C, an overpotential of −200 mV is required in order to reduce the surface concentration of the reactant to 0.1% of the bulk concentration. Thus the reduction of the Pb(II), Zn(II) and Mg(II) ions was studied potentiostatically by applying overpotentials between −200 and −300 mV. A linear relationship between i and $t^{-1/2}$ was found for Pb and Zn, and calculation of the diffusion coefficients with Equation 9 yielded $D_{Pb(II)} = 1.01 \times 10^{-5}$ cm^2 s^{-1} and $D_{Zn(II)} = 1.06 \times 10^{-5}$ cm^2 s^{-1}. The results are included in Table 1.

Whereas the value for $D_{Pb(II)}$ is in satisfactory agreement with those obtained by voltammetry, $D_{Zn(II)}$ is nearly 80% higher than the corresponding voltammetric results. Moreover, in the case of Mg(II) reduction, the plot of i against $t^{-1/2}$ was not even linear; nor did it pass through the origin. The reason for this is, of course, that the codeposition of alkali metals becomes increasingly more important at higher overpotentials, as illustrated by the sloping convolution voltammograms in Figure 5 and Figure 7. Generally speaking, the large currents arising from reduction of the solvent (or the supporting electrolyte) make electrochemical studies at potentials much more negative than their onset rather impractical [18]. In the present case it is consequently better to measure D at the voltammetric peak potential, where the alkali codeposition is relatively insignificant, than at overpotentials of several hundred millivolts.

3.4. *Temperature dependence of D*

The diffusion coefficients of the Pb(II), Zn(II) and Mg(II) ions in KCl–LiCl eutectic were determined at regularly spaced intervals between 400 °C and 500 °C. Their temperature dependence is illustrated by the Arrhenius plots in Figure 11. The linearity between ln D and T^{-1} is confirmed by the fact that the difference between each experimental point and its corresponding regression line does not exceed 3%.

From the slopes and intercepts of the regression lines, the following empirical expressions for $D(T)$ may be deduced:

$$D_{Pb(II)} = 5.294 \times 10^{-3} \exp\left(-\frac{35776}{RT}\right) \tag{10}$$

$$D_{Zn(II)} = 6.168 \times 10^{-3} \exp\left(-\frac{38781}{RT}\right) \tag{11}$$

$$D_{Mg(II)} = 4.166 \times 10^{-3} \exp\left(-\frac{33080}{RT}\right) \tag{12}$$

The activation energies for the diffusion processes are thus 35.8, 38.8 and 33.1 kJ mol^{-1}, respectively. As illustrated in Figure 11, the relative magnitudes of these

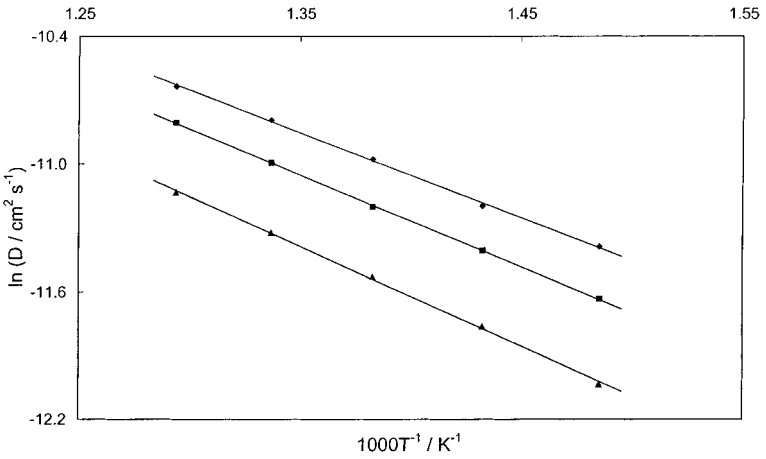

Fig. 11. Temperature dependence of $D_{Pb(II)}$, $D_{Zn(II)}$ and $D_{Mg(II)}$ in KCl–LiCl eutectic in the range 400–500 °C. Key: (◆) Mg, (■) Pb, (▲) Zn.

Table 2. Literature data for the diffusion coefficients of the Pb(II) and Zn(II) ions in KCl–LiCl

Authors	Experimental technique	t/°C	$10^5\ D_{Pb(II)}$/cm^2 s^{-1}	$10^5\ D_{Zn(II)}$/cm^2 s^{-1}
This work	CPSV/LSV	400	0.89	0.59
Thalmayer et al. [5]	Chronopotentiometry	400	0.89	
Naryshkin and Yurkinskii [6]	LSV	400	1.20*	
Yurkinskii and Makarov [8]	Chronopotentiometry	400	1.31*	
Kamaludeen et al. [12]	LSV	400		0.72†
This work	CPSV/LSV	450	1.37	0.99
Laitinen and Gaur [4]	Chronopotentiometry	450	2.18	
Thalmayer et al. [5]	Chronopotentiometry	450	1.3*	
Naryshkin and Yurkinskii [6]	LSV	450	1.75*	
Yurkinskii and Makarov [8]	Chronopotentiometry	450	1.85*	
Heus and Egan [9]	Polarography	450	1.7	
Schmidt [10]	AC polarography	450	2.2	1.1
This work	CPSV/LSV	500	2.03	1.46
Thalmayer et al. [5]	Chronopotentiometry	500	1.9*	
Naryshkin and Yurkinskii [6]	LSV	500	2.43*	
Sternberg et al. [7]	LSV	500	2.1‡	
Sternberg et al. [7]	Chronoamperometry	500	3.5	
Yurkinskii and Makarov [8]	Chronopotentiometry	500	2.50*	

* calculated with reported $D(T)$ equation
† calculated from reported i_p vs v data
‡ reported value recalculated with Equation 4

activation energies tend to decrease the differences between the diffusion coefficients at higher temperatures. Table 2 contains some relevant data from the literature. There is reasonable agreement between the $D_{Zn(II)}$ values, whereas the $D_{Pb(II)}$ values vary over a much wider range, the results of this work being in the lower end. No data on the diffusion of the Mg(II) ion in KCl–LiCl in this temperature range was found.

4. Conclusion

The diffusion coefficients of ions depositing on solid electrodes in molten chlorides have been determined by various electrochemical techniques. The preceding discussion may be summarized as follows. For processes with a large nucleation overpotential, CPSV is believed to be superior to LSV. The opposite conclusion applies if codeposition of alkali ions is significant, in which case the determination of the cathodic limit of the convolution voltammogram becomes difficult. Chronopotentiometry is inferior to voltammetry when it comes to correcting for residual currents. Determination of diffusion coefficients from single potential steps is not considered to be a very reliable method.

Acknowledgements

T.S. is grateful to the Research Council of Norway (NFR) for the award of an individual doctoral fellowship. Additional financial support was granted by NFR and Hydro Magnesium through the PROSMAT research programme.

References

1. T. Berzins and P. Delahay, *J. Am. Chem. Soc.* **75** (1953) 555.
2. M. Abramowitz and I.A. Stegun, 'Handbook of Mathematical Functions' (Dover Publications, New York, 1965).
3. G.J. Hills, D.J. Schiffrin and J. Thompson, *Electrochim. Acta* **19** (1974) 657.
4. H. Laitinen and H.C. Gaur, *Anal. Chim. Acta* **18** (1958) 1.
5. C.E. Thalmayer, S. Bruckenstein and D.M. Gruen, *J. Inorg. Nucl. Chem.* **26** (1964) 347.
6. I.I. Naryshkin and V.P. Yurkinskii, *Sov. Electrochem.* **5** (1969) 810.
7. S. Sternberg, T. Visan, N. Bonciocat and A. Cotărtâ, *Rev. Roumaine Chim.* **32** (1987) 883.
8. V.P. Yurkinskii and D.V. Makarov, *Russ. J. Appl. Chem.* **67** (1994) 1132.
9. R.J. Heus and J.J. Egan, *J. Electrochem. Soc.* **107** (1960) 824.
10. E. Schmidt, *Electrochim. Acta* **8** (1963) 23.
11. S.V. Mentus and M.V. Šušić, *J. Serb. Chem. Soc.* **50** (1985) 563.
12. M. Kamaludeen, K. Balakrishnan, G. Singh and N.S. Rawat, *B. Electrochem.* **4** (1988) 491.
13. J.C. Imbeaux and J.M. Savéant, *J. Electroanal. Chem.* **44** (1973) 169.
14. M. Grenness and K.B. Oldham, *Anal. Chem.* **44** (1972) 1121.
15 S.N. Flengas, *in* C.A. Hampel (ed.), 'The Encyclopedia of Electrochemistry' (Reinhold, New York, 1964), p. 644.
16. Y. Castrillejo, A.M. Martínez, R. Pardo and G.M. Haarberg, *Electrochim. Acta* **42** (1997) 1869.
17. R. Greef, R. Peat, L.M. Peter, D. Pletcher and J. Robinson, 'Instrumental Methods in Electrochemistry' (Ellis Horwood, Chichester, UK, 1990).
18. A.J. Bard and L.R. Faulkner, 'Electrochemical Methods. Fundamentals and Applications' (J. Wiley & Sons, New York, 1980).
19. A. Serruya, J. Mostany and B.R. Scharifker, *J. Chem. Soc. Faraday Trans.* **89** (1993) 255.